The results of Kolomoitsev *et al.* (6) are substantially in accord with this study. They reported calcium halophosphate phosphor as electroluminescent, along with other phosphors having zinc or cadmium as cations. They did not report on the relative brightness of the various phosphors. Apparently they did not use a solid dielectric film in their cells. They introduced the phosphor directly between a metal plate and conducting glass.

Palilla and Rinkevics (7) examined a number of phosphors activated by rare earths, as well as alumina activated by Cr or Mn. In general, their observations on what they called Type II emission were similar to those observed by the author in self-activated tungstates and in binary oxides activated by Mn or by Pb + Mn. The effects of frequency and of liquid embedment were similar in both investigations. However, they found it necessary to provide a special thermal treatment of their phosphors, while the author gave no special treatment to the phosphors he examined.

Conclusions

Many oxide phosphors exhibit electroluminescence, giving light outputs equal to sulfide phosphors at about the same current, but at about 20 times the voltage and 20 times the wattage.

Electroluminescence in oxide phosphors is believed to be due to bombardment of the phosphor by electrons or ions or to recombination of charged particles on or near the phosphor surface. Bombardment may occur at an air-phosphor interface or at a semiconductor-phosphor interface, depending on cell construction. Photoluminescence plays a negligible role in the cells described.

Oxide phosphors with zinc or cadmium as the metallic cation are in general more efficient than those with calcium or strontium.

The threshold voltage required for EL in oxide phosphors is reduced by providing contacts between the phosphors and cadmium pyroantimonate semiconductor grains. Such contacts also make oxide EL cells operable in high vacuum.

The existence of electroluminescent oxide phosphors as efficient as sulfides does not seem an impossibility. Crystal aggregates containing both electron-emitting and fluorescent phases would seem to have electroluminescent potentialities in oxide systems.

Acknowledgment

The assistance of Herman Ogrinc in this project is gratefully acknowledged.

Manuscript received Aug. 29, 1963.

Any discussion of this paper will appear in a Discussion Section to be published in the December 1964 JOURNAL.

REFERENCES

1. Willi Lehmann, *This Journal*, **104**, 45 (1957).
2. O. W. Lossew, Telegrafia i Telefonia, **18**, 61 (1923).
3. G. Destriau, *J. chim. phys.*, **33**, 620 (1936); **34**, 117 (1937).
4. H. F. Ivey, *This Journal*, **104**, 740 (1957).
5. J. N. Bowtell and H. C. Bate, *Proc. Inst. Radio Engrs.*, **44**, 697 (1956).
6. F. I. Kolomoitsev, V. P. Izotov, and E. V. Stauer, *Optics and Spectroscopy*, **12**, 64 (1962).
7. F. C. Palilla and M. Rinkevics, *This Journal*, **110**, 750 (1963).
8. A. Herwelly, *Acta Phys. Austriaca*, **5**, 30, (1951).
9. L. Thorington, Paper presented at Electrochemical Society Meeting, Philadelphia, 1952 (Abstract 52).
10. B. Morosin and F. A. Haak, *This Journal*, **108**, 477 (1961).
11. W. Lehmann, *ibid.*, **109**, 540 (1962).
12. A. Addamiano, Private discussion.

Spectral Properties of Rare Earth Oxide Phosphors

R. C. Ropp[1]

Sylvania Electric Products Inc., Towanda, Pennsylvania

ABSTRACT

A study of rare earth oxide phosphors activated by rare earths revealed that fluorescence occurs only in those matrices where the cation possesses no unpaired electrons. The fluorescent intensities of the rare earth activators were divided into three categories, strong, medium, and weak, each having a characteristic excitation spectrum.

The study of spectral properties of rare earth activated phosphors is fundamental for an understanding of the luminescence process. In the rare earths, transitions among the f-electron energy levels result in line emission because the outer shielding electrons ($5s^25p^6$) minimize the perturbing influence of the crystal field. In the more usual case involving d-electrons, considerable perturbation occurs, resulting in broad emission bands.

The general field of oxide phosphors has been long neglected because of the low fluorescent intensities associated with such phosphors. Bonding involves a high degree of ionic character, and activators in which d-electron transitions take place do not produce high-intensity fluorescence. In such ionic solids, the excitation energy required for fluorescence at the d-electron activator site probably is dissipated in part by phonon processes via vibronic coupling or by spin-orbit exchange. However, with f-electrons, such a process should be minimized

[1] Present address: Westinghouse Electric Corporation, Bloomfield, New Jersey.

and thus permit the oxide-matrix combination with rare earth activation to produce phosphors of higher efficiency.

The rare earths form a series of homologous oxides having a cubic defect structure (1, 2). The state of present knowledge regarding the specific transitions involved in rare earth excitation and fluorescence is not extensive, nor is the nature of the transitions well defined. However, the energy levels of the tervalent ions are known quite well, the identification of the levels (SLJ) being complete in most cases up to 40,000 cm^{-1} (3). The correlation between the free ion levels and observed levels in a crystal is quite close, of the order of 100 cm^{-1}, in contrast with those of d-electron activators.

A study of rare earth activated, rare earth oxide phosphors was initiated to study activator matrix interactions and to elucidate the luminescent mechanisms of the rare earths as activators. Such a choice minimizes experimental difficulties to a certain degree.

Previously known phosphors include: $Gd_2O_3:X^{+3}$, where X^{+3} is Sm, Eu, or Tb(4); $Y_2O_3:X^{+3}$, where X^{+3} is Eu, Tb, Pr, Dy, or Er (5), and Sm (6); $CeO_2:X^{+3}$, where X^{+3} is Sm, Gd (6); and La_2O_3:Pr (7).

Experimental Procedure

All materials were at least 99.99% pure. Impurities other than rare earths were not detected spectrographically. The nitrates (or the oxides dissolved in concentrated nitric acid) of the requisite rare earths were dissolved to form 0.40M solutions. Mixtures of the ions in solution were made so that the required volumes totaled one liter before precipitation. The activator ratio was 0.05 mole/mole of Gd^{+3}, Y^{+3}, $La,^{+3}$, or other desired cation, so that in the total volume, the ratio of activator to cation remained constant. Oxalic acid as a 10% solution was used as the precipitant, assuming the reaction to be quantitative in the presence of 5M % excess acid (8)

$$2M^{+3} + 3(HOC(=O)-C(=O)OH) \rightarrow M_2(HOCCOH)_3 \cdot XH_2O$$

where $X = 2$ to 6 when the precipitation is carried out at 80°C. The precipitate was dried at 110°C overnight and fired in air at 1000°C to form the phosphor, using open silica crucibles.

Measurements of spectral properties were made with a spectrofluorimeter described previously (9). Only visible fluorescence, and in one case ultraviolet emission, was measured. No attempt to measure luminescence below 14,400 cm^{-1} (6940Å) was made. It is probable that infrared emission occurs in many, if not all, of the phosphors. This aspect was not of interest in the present investigation.

Experimental Results

In general, calcination of the rare earth oxalate gave the rare earth sesquioxide. In the case of Ce and Pr, CeO_2 and Pr_6O_{11} were formed when the corresponding oxalates were fired in air. However, when fired in N_2, they gave the expected sesquioxide (10). The experimental investigation was conducted in three steps: determination of effective matrices; investigation of spectral properties; and correlation of excitation and emission properties.

Effective Matrices

To ascertain the effective rare earth activator-rare earth oxide combinations and yet not exceed the bounds of experimental feasibility, it was necessary to restrict the choice of possible activators. In a study of rare earth-activated Al_2O_3, Adams and Mellickamp (11) found that only Sm^{+3}, Eu^{+3}, Gd^{+3}, Tb^{+3}, and Dy^{+3} were effective. It is also well known (12) that these same rare earth activators produce much higher intensities of fluorescence than any of the other rare earths. Therefore, limiting the choice to these five activators could be justified experimentally; it is unlikely that any other rare earth activator would produce significantly different results.

Fluorescence was evaluated by its presence or absence. The wave-number range, 14,400 cm^{-1} to 45,500 cm^{-1}, was scanned to determine if excitation was obtained. The data in Table I were obtained in this manner. The fluorescent intensities varied, by a factor of ten, from weak to strong.

The oxides were identified by x-ray powder diffraction patterns of the activated phosphors. Note that only Y_2O_3, La_2O_3, and Gd_2O_3 gave activated matrices. There is a correlation between activation, electron configuration, and body color (Table II). In the effective matrices, there are no unpaired spins, and the body color is white, *i.e.*, no absorption

Table I. Visible fluorescence in the rare earth oxide matrices

Matrix	Structure	Activator* Sm^{+3}	Eu^{+3}	Gd^{+3}	Tb^{+3}	Dy^{+3}
Y_2O_3	Cubic	w	s	w	m	m
La_2O_3	Hexagonal	w	s	m	s	m
Ce_2O_3**	Hexagonal	—	—	—	—	—
Pr_2O_3†	Hexagonal	—	—	—	—	—
Nd_2O_3	Hexagonal	—	—	—	—	—
Sm_2O_3	Monoclinic	—	—	—	—	—
Gd_2O_3	Cubic	w	s	—	s	m
Dy_2O_3	Cubic	—	—	—	—	—
Ho_2O_3	Cubic	—	—	—	—	—
Er_2O_3	Cubic	—	—	—	—	—
Yb_2O_3	Cubic	—	—	—	—	—

* w = weak; m = medium; s = strong intensity.
** Fired in N_2. Firing in air produces cubic CeO_2 which has the fluorite structure.
† Fired in N_2. Firing in air produces the cubic Pr_6O_{11}.

Table II. Correlation of visible luminescence, electron configuration, and body color

Matrix	Activation obtained	Outer electron configuration		No. of unpaired spins	Body color
Y_2O_3	X	$4f^0$	$4s^24p^6$	0	White
La_2O_3	X	$4f^0$	$5s^25p^6$	0	White
Ce_2O_3		$4f^1$	$5s^25p^6$	1	White
Pr_2O_3		$4f^2$	$5s^25p^6$	2	Green
Nd_2O_3		$4f^3$	$5s^25p^6$	3	Blue
Sm_2O_3		$4f^5$	$5s^25p^6$	5	Cream
Gd_2O_3	X	$4f^7$	$5s^25p^6$	7	White
Dy_2O_3		$4f^9$	$5s^25p^6$	2	Cream
Ho_2O_3		$4f^{10}$	$5s^25p^6$	3	Pink
Er_2O_3		$4f^{11}$	$5s^25p^6$	4	Pink
Yb_2O_3		$4f^{13}$	$5s^25p^6$	6	White

in the visible region, whereas in those matrices where unpaired electrons exist, no visible luminescence was observed. This is exactly what would be expected, since the presence of an unpaired electron implies the presence of low-lying energy levels. Cations with a closed-shell electron configuration require very high ionization energy, and no low-lying levels will be present. In the case of two or more electrons, it is unusual to find spin-pairing, except in the presence of a strong crystal field (13). Thus, in the rare earth oxides with unpaired 4f electrons, many low-lying levels are present and absorption occurs in the visible region. Excitation energy is easily dissipated or results in infrared emission. The special stability of a half-filled electron shell is well recognized and for Gd^{+3} results in only a few energy levels between 0 and 40,000 cm^{-1} (3). Activation was obtained only in the matrices where the cation has no unpaired electrons, *i.e.*, no angular momentum and no low-lying energy levels, thus minimizing interaction of the activator site with the matrix.

Effective Activators

Using the three oxides, La_2O_3, Y_2O_3, and Gd_2O_3, as matrices, fluorescent properties of the rare earth activators were investigated. In previous investigations, Dieke and his co-workers (14) have found that most of the rare earths produce luminescence in $LaCl_3$. In the present case, not all of the rare earths, when incorporated in oxide matrices, give rise to fluorescence. The results found are given in Table III. Ultraviolet excitation was obtained by scanning the wave-length range until maximum response was found.

The results obtained parallel those obtained by previous investigators (8, 12) concerning fluorescent intensities of rare earths. Thus, Sm^{+3}, Eu^{+3}, Gd^{+3}, Tb^{+3}, and Dy^{+3} gave the highest fluorescent response to ultraviolet excitation, which was varied between 14,400 cm^{-1} and 45,500 cm^{-1} in order to evaluate the luminescence properties. The intensities differed by a factor of ten between weak and strong intensities.

Excitation-Emission Properties

The spectral properties were measured using a commercial radiometer (9). In all cases, the excitation spectrum of the strongest emission line was measured, and then the emission lines were remeasured to determine if change in excitation wave length induced a change in emission lines. Only visible fluorescence was measured. Thus, the transition of Er^{+3} from its lowest fluorescent state, according to Dieke and Singh (15), would occur at 11,900 cm^{-1} (8440Å), a region which was not evaluated for fluorescence. The spectra are all normalized. The excitation beam was maintained at constant energy. The band pass of the instrument in the ultraviolet was about 2-10Å, depending on wavelength. Thus, spectral accuracy was believed to be within 100 cm^{-1} of the true values.

High-intensity emission.—High-intensity emission was observed with the activators Eu^{+3} and Tb^{+3}. The strongest line for Eu^{+3} is at 16,100 cm^{-1} in La_2O_3, and at 16,400 cm^{-1} in Y_2O_3 and Gd_2O_3, as shown in Fig. 1. The excitation spectra consist of broad bands with some lower intensity structure. The spectral properties are tabulated in Table IV for the main excitation bands and emission lines for each activator, exclusive of the levels attributable to transitions within the 4f configuration (ionic levels).

The emission lines were found to be nearly the same, but the excitation bands differed considerably. Because the 43,800 cm^{-1} band in La_2O_3 phosphors appears in all cases, regardless of activator (see below), it is probably a matrix excitation band. Ex-

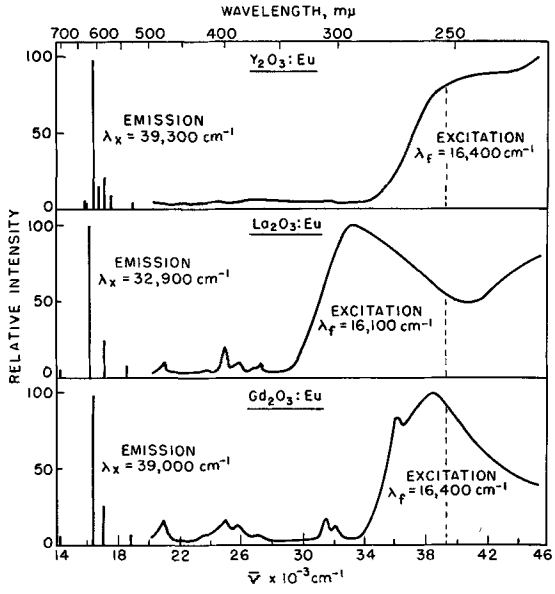

Fig. 1. Fluorescence of Eu^{+3} in rare earth oxide matrices

Table III. Activation in La_2O_3, Y_2O_3, and Gd_2O_3 matrices

Activator	Ground state	Matrix		
		La_2O_3	Gd_2O_3	Y_2O_3
Ce^{+3}	$^2F_{5/2}$	—	—	—
Pr^{+3}	$^3H_4$	m	—	—
Nd^{+3}	$^4I_{9/2}$	—	—	—
Sm^{+3}	$^6H_{5/2}$	w	w	w
Eu^{+3}	$^7F_0$	s	s	s
Gd^{+3}	$^8S_{7/2}$	m	—	w
Tb^{+3}	$^7F_6$	s	s	m
Dy^{+3}	$^6H_{15/2}$	m	m	m
Ho^{+3}	$^5I_8$	w	—	w
Er^{+3}	$^4I_{15/2}$	w	—	w
Tm^{+3}	$^3H_6$	w	—	—
Yb^{+3}	$^2F_{7/2}$	—	—	—
Lu^{+3}	$^1S_0$	—	—	—

Table IV. Spectral properties of Eu^{+3} and Tb^{+3} in rare earth oxide matrices

	Matrix					
	La_2O_3		Y_2O_3		Gd_2O_3	
	Emission, cm^{-1}	Excitation, cm^{-1}	Emission, cm^{-1}	Excitation, cm^{-1}	Emission, cm^{-1}	Excitation, cm^{-1}
Eu^{+3}	16,100	33,500 44,000	16,400	41,500 >46,000	16,400	36,100 38,600
Tb^{+3}	18,400	36,500 43,800	18,400	32,700 35,600	18,300	33,200 43,200

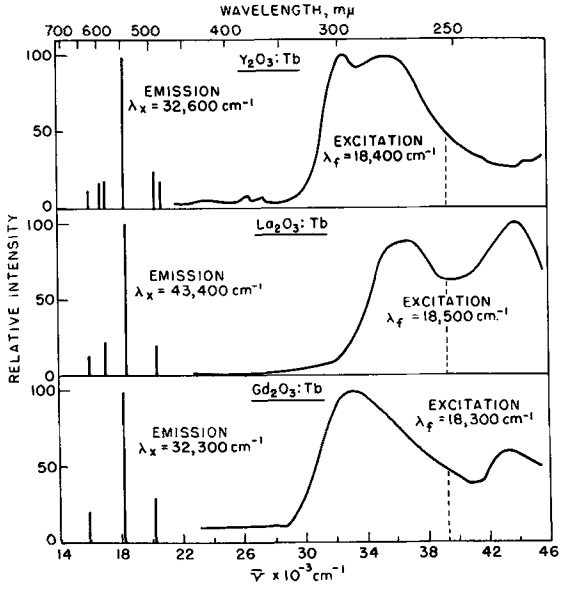

Fig. 2. Fluorescence of Tb^{+3} in rare earth oxide matrices

citation of the La_2O_3 matrix produced the same fluorescence as excitation in the lower intensity energy levels of the ionic activator. Excitation of the ionic levels of Eu^{+3} (transitions within the 4f configuration) was obtained in all cases, but excitation of Tb^{+3} ionic energy levels, for the most part, was absent, as shown in Fig. 2. The excitation spectrum of Y_2O_3 is suggestive of a band beyond the limits of measurement, and this hypothesis was confirmed by separate measurement (16). The second excitation band appears at 50,000 cm^{-1}. The rather narrow peak at 36,200 cm^{-1} in Gd_2O_3:Eu can be correlated to an excitation of the ^6I_J levels of the Gd^{+3} ion. This peak appears in most phosphors involving the Gd_2O_3 matrix.

Thus, for those phosphors having intense emission, fluorescence occurs by excitation which produces transitions within the 4f configuration, host lattice excitation (host sensitization) or excitation in an intense broad energy band which is probably related to a perturbed level of the activator. This band may be contrasted with the aforementioned rather narrow low-energy excitation bands which represent nonperturbed 4f transitions.

Medium intensity emission.—Medium intensity fluorescence was observed for the activators Sm^{+3}, Dy^{+3}, and Pr^{+3}, depending on the matrix. For Dy^{+3}, the spectra shown in Fig. 3 can be again divided into separate phenomena. The rather narrow excitation bands are associated with nonperturbed 4f transitions. The main emission lines and excitation peaks for La_2O_3:Dy, Gd_2O_3:Dy, and Y_2O_3:Dy, exclusive of ionic levels, are shown in Table V, as well as those for La_2O_3:Sm (see Fig. 3).

In La_2O_3, the matrix excitation band appears at 43,500 cm^{-1} in addition to the $4f^n$ excitation transitions. Both give rise to the main emission line of Dy^{+3} at 17,500 cm^{-1}. Those phosphors based on the La_2O_3 matrix generally produced phosphors of medium intensity emission.

In Y_2O_3, the matrix excitation band is not in a measured range, so that the main excitation peak indicated is a transition within the $4f^n$ configuration.

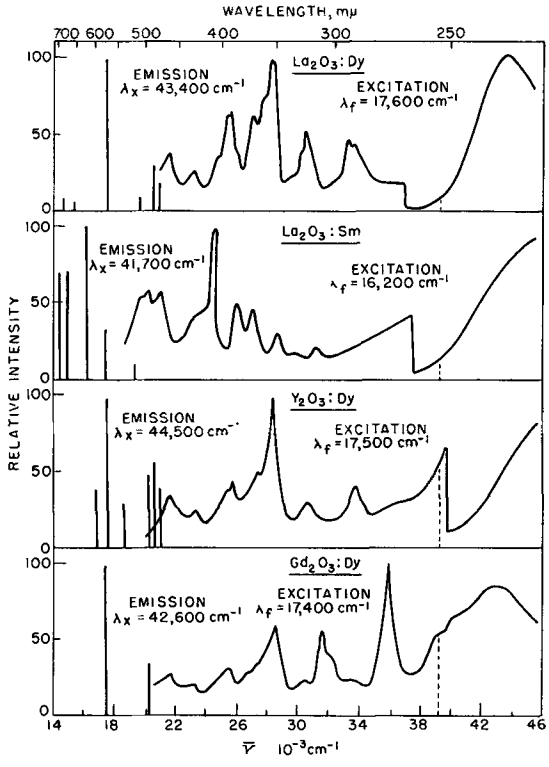

Fig. 3. Fluorescence of Dy^{+3} in rare earth oxide matrices

In Gd_2O_3, there is a broad excitation band, apparently belonging to the matrix, but the strongest excitation band belongs to the ^6I levels of Gd^{+3} (3). There are Gd^{+3} ionic levels superimposed on the broad excitation band at 39,100 cm^{-1} and 40,200 cm^{-1}. These are probably ^6D_J levels superimposed on the matrix excitation band. Thus, in this case, two types of excitation bands can be identified, nonperturbed $4f^n$ transitions and matrix excitation bands, but not the perturbed band involving one of the excited states of the activator found for the intense emitters.

Pr^{+3}.—Pr^{+3} in La_2O_3 leads to a medium intensity phosphor with the typical broad band perturbed level, probably associated with a Pr^{+3} excited state. In addition, the matrix excitation band is present at 43,600 cm^{-1} (see Fig. 7). The strongest fluorescence line is at 19,600 cm^{-1}.

Weak intensity emission.—The systems which are relatively weak in emission intensity are those in which only $4f^n$ transitions are involved and little perturbation is evident.

Gd^{+3}.—In La_2O_3, medium intensity is observed because host excitation occurs additionally (see

Table V. Spectral properties of Dy^{+3} in rare earth oxide matrices

	Matrix					
	La_2O_3		Y_2O_3		Gd_2O_3	
	Emission, cm^{-1}	Excitation, cm^{-1}	Emission, cm^{-1}	Excitation, cm^{-1}	Emission, cm^{-1}	Excitation, cm^{-1}
Dy^{+3}	17,500	43,500				
	19,400	35,700	17,500	44,500	17,400	43,000
Sm^{+3}	16,200	44,000	Too weak to measure			
Pr^{+3}	19,600	43,600	none		none	

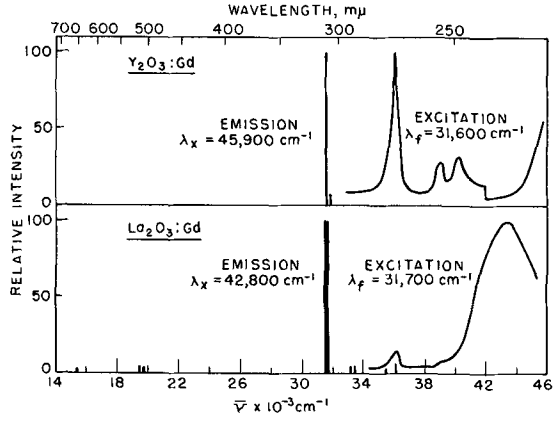

Fig. 4. Fluorescence of Gd^{+3} in rare earth oxide matrices

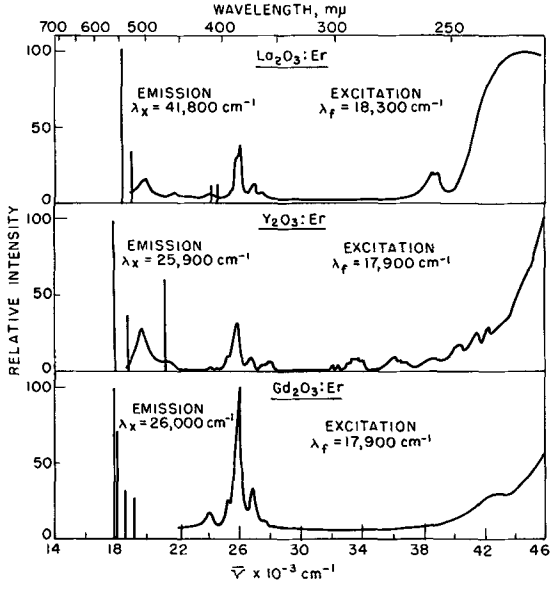

Fig. 5. Fluorescence of Er^{+3} in rare earth oxide matrices

Fig. 4). In Y_2O_3:Gd, the main excitation band is the Gd^{+3} triplet level, Table VI. This gives rise to the ultraviolet line emission. Thus, weak emission intensity is again associated with the absence of a perturbed excitation state of the activator.

Er^{+3}.—The emission intensity associated with Er^{+3} activator is always weak. The spectra are given in Fig. 5. In La_2O_3, excitation in the matrix band does not produce intense emission. Aparently, the host sensitization process is not efficient, and the resonance coupling is not strong between cation sites and activator. The transfer of energy would be expected to occur by resonant states of the matrix and activator (exciton states and excited dipole states). In Y_2O_3, the emission lines of Er^{+3} are extremely weak and differ slightly from those found for Er^{+3} in La_2O_3. The excitation spectrum shows considerable structure. The ionic excitation levels are very weak, and there is no matrix excitation in the range measured. In Gd_2O_3, a similar situation prevails, except that the ionic levels are much more intense. The ^6I state of Gd^{+3} is absent, indicating that host lattice resonance coupling, while stronger than Y_2O_3, is not very efficient, and that the sensitization process is not strong. There is a band at 43,000 cm^{-1}, indicative of host matrix excitation, but it is extremely weak. The main excitation and emission lines of Er^{+3} are summarized in Table VII, which includes the properties of Ho^{+3} in the same matrices (see Fig. 6).

The spectra of Er^{+3} in rare earth oxides consist of many interconfiguration transitions involved in excitation and emission.

For Ho^{+3} in the rare earth oxides, the emission intensity is also weak compared with other activators. In La_2O_3, the usual matrix excitation band is present, and the coupling, *i.e.*, sensitization, seems to be somewhat stronger than for Er^{+3} in the same matrix. In Gd_2O_3, an excitation state of Ho^{+3} is seen which is not present in the La_2O_3 phosphor. Further study of these phosphors is necessary to determine the effect of structure on relative intensity of the $4f^n$ excitation transitions.

Tm^{+3}.—In La_2O_3, Tm^{+3} gives a single blue emission line at 21,700 cm^{-1} and a resonance line at 27,000 cm^{-1} (Fig. 7). The intensity is very low. Excitation in the matrix band yields these emission lines, but

Table VI. Spectral properties of Gd^{+3} in rare earth oxide matrices

	Matrix			
	La_2O_3		Y_2O_3	
	Emission, cm^{-1}	Excitation, cm^{-1}	Emission, cm^{-1}	Excitation, cm^{-1}
Gd^{+3}	31,600) 31,700) 19,600	43,400 35,000	31,600	36,200
Intensity	medium		weak	

Table VII. Spectral properties of Er^{+3} in rare earth oxide matrices

	Matrix					
	La_2O_3		Y_2O_3		Gd_2O_3	
	Emission, cm^{-1}	Excitation, cm^{-1}	Emission, cm^{-1}	Excitation, cm^{-1}	Emission, cm^{-1}	Excitation, cm^{-1}
Er^{+3}	17,900	21,700 26,000 14,000	17,900	19,700 25,900	17,900	24,100 26,100 27,000 43,000 (w)
Intensity	weak		weak		weak	
Ho^{+3}	18,000	19,800) 21,200) 43,400	18,200	21,100) 21,600) 21,900)	18,100	20,100) 20,700) 27,300) 43,000 (w)
Intensity	weak		weak		weak	

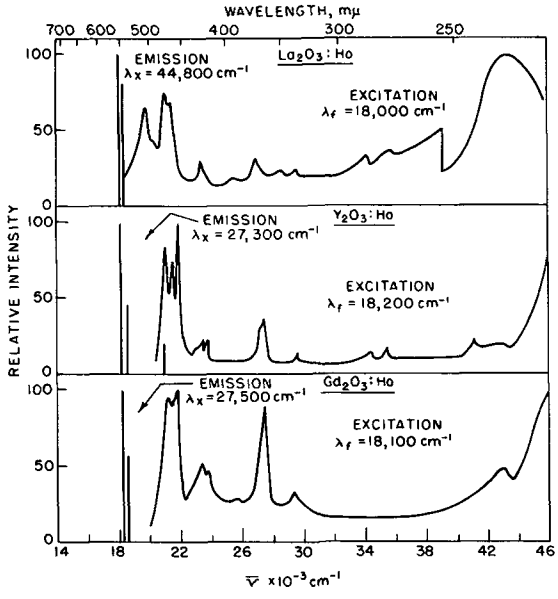

Fig. 6. Fluorescence of Ho^{+3} in rare earth oxide matrices

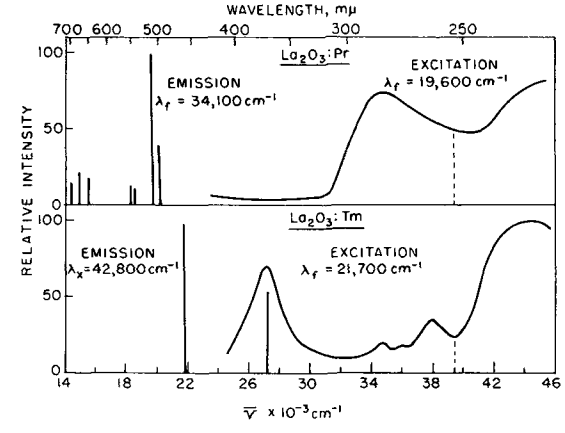

Fig. 7. Fluorescence of Pr^{+3} and Tm^{+3} in rare earth oxide matrices

the ionic levels are too weak to produce enough energy for measurement, except for the resonance line.

Conclusions

It has been shown that fluorescence is present in these systems where the cationic matrix component possesses the inert gas electron configuration (ns^2np^6). This corresponds to the case for d-electron activators. Since line spectra are observed, it is probable that perturbation of the emitting state is not large.

Correlation of the excitation spectra shows that the phosphors in each of the three emission intensity categories possess characteristic excitation spectra. For the weak emitters, only $4f^n$ configuration excitation transitions were noted. For the medium intensity phosphors, host sensitization seems to be the primary mechanism, but weak $4f^2$ excitation transitions were also present. For the intense emitters, the broad perturbed band, probably representing an excited state of the activator, predominates over all other features. Thus, intensity is associated with degree of perturbation.

The fundamental question of the origin of the broad excitation bands, other than those attributed to matrix excitation bands, is a difficult one, since excitation of Eu^{+3} or Tb^{+3} could involve either intraconfiguration transitions, as is more common in the d-electron activators, *i.e.*, changes in angular momentum, or transitions within the same configuration, the excited state of which is perturbed by the crystal field. The emitting state most certainly involves a $4f^n$ energy level, but it has become obvious (10) that the excitation and emission states are not one and the same. The excited states involve SLJ states which could belong either to the $4f^{n-1}$ 5d or $4f^n$ configurations. If the former possibility prevailed, then one would expect line broadening in emission. This was not observed. The possibility that a transition between one of the excited states of the $4f^{n-1}$ 5d configuration and a metastable state of the $4f^n$ configuration could occur prior to emission appears unlikely. Thus, the broad intense excitation band is probably associated with an excited state of the $4f^n$ configuration perturbed by the crystal field. Recently, Dieke and Crosswhite (3) have estimated the positions of the $4f^{n-1}$ 5d states of the tervalent rare earths to be above 50,000 cm^{-1}. If this estimate is correct, then there is little ambiguity as to the origin of the intense excitation bands found for Eu^{+3} and Tb^{+3}. The reasons for the unique behavior of these activators in a cation site of C_{3v} symmetry (c-type rare earth oxide) have not been explained. The logical choice to explain the nature of the high-intensity fluorescent transitions seems to be "induced electric dipole" transitions in which the selection rule becomes nonvalid when the nucleus of the activator is situated at a site whose symmetry lacks a center of inversion (17).

Acknowledgment

The author wishes to thank Dr. R. W. Mooney for his advice and encouragement, and H. D. Layman for preparation of the materials.

Manuscript received June 12, 1963; revised manuscript received Sept. 23, 1963.

Any discussion of this paper will appear in a Discussion Section to be published in the December 1964 JOURNAL.

REFERENCES

1. I. Warshaw and R. Roy, *J. Chem. Phys.*, **65**, 2048 (1961).
2. L. Pauling and M. D. Shappell, *Z. Krist.*, **75**, 128 (1930).
3. G. H. Dieke and H. M. Crosswhite, *Appl. Optics*, **2**, 675 (1963).
4. G. Urbain, *Ann. chim. phys.*, **18**, 293 (1909).
5. K. L. Wickersheim and R. A. La Fever, Unpublished data.
6. R. Tomaschek, *Z. Elektrochem.*, **36**, 737 (1930).
7. H. Gobrecht and R. Tomaschek, *Ann. Phys.*, **29**, 324 (1937).
8. K. G. Broadhead and H. H. Heady, *Anal. Chem.*, **32**, 1603 (1960).
9. W. Slavin, R. W. Mooney, and D. T. Palumbo, *J. Opt. Soc. Am.*, **51**, 93 (1961).
10. R. C. Ropp, Unpublished data.
11. I. Adams and J. W. Mellickamp, *J. Chem. Phys.*, **36**, 2456 (1962).

12. K. Hellwege, *Ann. Phys.*, **40**, 529 (1942).
13. D. S. McClure, "Solid State Phys.," Vol. 9, F. Seitz and D. Turnbull, Editors, Academic Press, New York (1959).
14. G. H. Dieke and R. Sarup, *J. Chem. Phys.*, **36**, 371 (1962); F. Varsanyi and G. H. Dieke, *ibid.*, **31**, 1066 (1959); F. Varsanyi and G. H. Dieke, *ibid.*, **36**, 835 (1962); H. M. Crosswhite and G. H. Dieke, *ibid.*, **35**, 1535 (1961).
15. G. H. Dieke and S. Singh, *ibid.*, **35**, 555 (1961).
16. J. E. Eby, Private communication.
17. B. R. Judd, *Phys. Rev.*, **127**, 750 (1962).

The Dependence on Deposition Conditions of the Dopant Concentration of Epitaxial Silicon Layers

R. Nuttall

Ferranti Ltd., Wythenshawe, Manchester, England

ABSTRACT

Methods of doping epitaxial silicon layers produced by the hydrogen reduction of silicon tetrachloride are discussed, and a technique by which a constant concentration of dopant in the silicon tetrachloride vapor may be achieved is described. A function termed the conversion efficiency, η, is estimated for the various reactions taking place in the deposition cell, and the influence of various reaction conditions on η for several dopants are reported. The uniformity of dopant concentration in the epitaxial layers is discussed and methods for controlling the concentration gradient present at the substrate/epitaxial interface are indicated.

The epitaxial growth of silicon has been of particular interest in the silicon device field in view of the great potentialities of this technique. The most popular method by which epitaxial deposition is carried out is the hydrogen reduction of silicon tetrachloride, and the experiments described here were performed with a view to observing the influence of deposition conditions on the various reactions which take place during the deposition of doped silicon using this reaction.

Apparatus

The apparatus used in these experiments is similar to that described by Theuerer (1) and is shown in the flow diagram Fig. 1. The basic materials used in the construction are quartz and "Teflon." The hydrogen flow is controlled by tap T_1 which allows hydrogen to pass directly into the cell and tap T_2 which allows the hydrogen to pass through an evaporator filled with $SiCl_4$ and contained in a thermostatic bath. Tap T_4 allows the gas to run to waste for a period during which the flow is stabilized, while T_3 directs the flow into the deposition cell. By operating the thermostatic bath at various temperatures and varying the relative flow rates a large range of molar ratios $SiCl_4/H_2$ may be obtained. The deposition cell is constructed from quartz, and the pedestal is prepared from high purity graphite over which is placed a quartz cap. The graphite used was grade AGW obtained from British Acheson Electrodes Ltd., England.

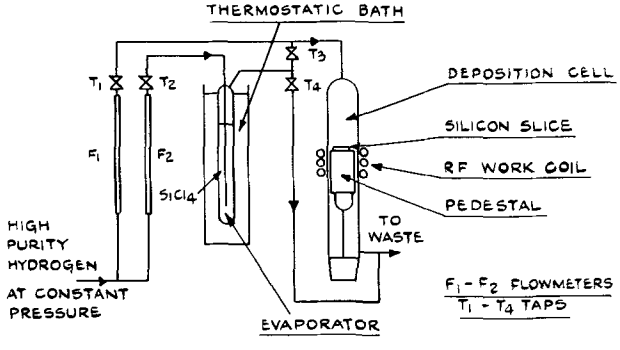

Fig. 1. Schematic flow diagram of equipment

The silicon slices used as substrates for the depositions were cut at 90° to the 111 axis and diamond polished, the final polishing being carried out using $\frac{1}{4}\mu$ particle size. The slices were cleaned by initially swabbing them with cotton wool soaked in methylene chloride followed by several rinses in clean methylene chloride. They were then dried using a clean dry nitrogen blast. Immediately before introducing each slice into the cell it was given a 2 min dip in hydrofluoric acid followed by several rinses in deionized water. It was then again dried with the nitrogen blast.

The mean resistivity of the epitaxial layers produced was calculated from four probe measurements and junction depth measurements, the latter being determined by the lapped bevel technique. In the system used the mean resistivity of the epitaxial layer deposited was found to be relatively independent of the substrate resistivity and type. However, in view of the possibility of gross contamination of the epitaxial layer by the substrate dopant reported by Basseches *et al.* (2), relatively high resistivity silicon of approximately 1-10 ohm-cm and of opposite conductivity type to the layer deposited was selected for the substrate. The conditions under which one may expect appreciable dopant transfer from the substrate are in fact suggested from the data obtained during these experiments. Each substrate was heated to 1250° in a